Collapse of Telechelic Star Polymers to Watermelon Structures

Federica Lo Verso, Christos N. Likos, Christian Mayer, and Hartmut Löwen
Institut für Theoretische Physik II, Heinrich-Heine-Universität Düsseldorf, D-40225 Düsseldorf, Germany
(Received 18 January 2006; published 9 May 2006)

Conformational properties of star-shaped polymer aggregates that carry attractive end groups, called telechelic star polymers, are investigated by simulation and analytical variational theory. We focus on the case of low telechelic star polymer functionalities, $f \leq 5$, a condition which allows aggregation of all attractive monomers on one site. We establish the functionality- and polymerization-number dependence of the transition temperature from the ''star burst'' to the ''watermelon'' macroparticle structure. Extensions to telechelic stars featuring partially collapsed configurations are also discussed.

DOI: 10.1103/PhysRevLett.96.187802 PACS numbers: 36.20.Ey, 61.20.Ja, 61.25.Hq, 82.70.Uv

Self-organizing soft materials are relevant in developing novel macromolecular compounds with peculiar structural and dynamical properties, related to mesoscopic aggregation as well as intramolecular and intermolecular association [1,2]. Progress in the synthesis of chains with attractive end groups, called functionalized or telechelic polymers, has opened the way for the subsequent synthesis of telechelic star polymers with attractive polar end groups, telechelic associating polymers with hydrophobic terminal groups, associating polyelectrolytes in homogeneous solutions, and telechelic planar brushes [3–6]. A telechelic star, subject of this work, consists of f chains with one end chemically attached on a common center, whereas the attractive opposite ends are free. Block-copolymer stars with a hydrophilic core and a hydrophobic corona [7,8] also bear similarities to telechelic stars when the length of the hydrophobic block reduces to few monomers. The thermodynamics and the structure of planar telechelic brushes have been recently analyzed also from a theoretical point of view, shedding light into the quantitative characteristics of both the conformations and the interactions of the same [9–11]. Further theoretical approaches have been developed to describe flowerlike micelles with hydrophobic terminal groups that self-assemble in water. Such aggregates show a characteristic ''bridging attraction'' [9,12] that can lead to a liquid-vapor phase transition [13]. The interesting feature of telechelic star polymers is the possibility of attachment between the attractive terminal groups. In dilute solutions, this yields intramolecular association as well as interassociation between micelles, depending on the details of the molecular structure.

Examples of low-functionality telechelics, very similar to the ones considered in this work, are mono-, di-, and tri-ω-zwitterionic, three-arm star symmetric polybutadienes. These starlike samples can be easily synthesized and provide a good means to study the balance between several kinds of interactions, controlled by an accessible number of parameters. Experiments have shown that these self-assemble into distinct supramolecular structures, including collapsed, soft-sphere conformations [4,14]. By using low-angle laser light scattering and dynamic light scattering, it was found that samples with three-zwitterion end groups present a low degree of interassociation between macromolecules, showing instead a preference for intra-association [3,15]. X-ray scattering and rheological experiments support the conclusion that this tendency persists at higher concentrations, all the way into the melt [4]. There, the formation of transient gels has been found for two- and three-zwitterion macromolecules, with the network characteristics depending on the molecular weight of the arms [14].

The conformations of telechelic micelles are determined by the competition between entropic and energetic contributions. A detailed investigation, by theory and simulation, of the mechanisms leading to the formation of collapsed soft spheres is, however, still lacking. In this Letter we perform extensive computer simulations, accompanied by a scaling analysis of the free energies of candidate structures of telechelic micelles with small functionality, $f \leq 5$. We find that at high temperatures the system assumes the usual star burst (sb) configuration. On the other hand, at sufficiently low temperatures, the end monomers attach to each other and the micelles assume an overall closed configuration, akin to the collapsed soft spheres conjectured in the experimental study of Ref. [4]. Because of the peculiar shape of these aggregates, featuring two points of aggregation, one at each end, we term them ''watermelons'' (WM). At a given, sufficiently low T, the WM configuration becomes more stable with respect to the sb one with decreasing N and increasing f. Our theoretical predictions agree well with simulation results and trends evidenced in experiments on tri-ω-zwitterionic macromolecules.

We employed monomer-resolved molecular dynamics (MD) simulations to examine the conformations of isolated telechelic micelles. The monomers were modeled as soft spheres interacting by means of a truncated and shifted Lennard-Jones potential, $V_{\mathrm{LJ}}^{\mathrm{tr}}(r)$ (length scale σ_{LJ}, energy scale ε), the truncation point being at the minimum, $r_{\mathrm{min}} = 2^{1/6}\sigma_{\mathrm{LJ}}$, rendering the interaction purely repulsive. The *end monomers*, on the other hand, interact with each other by means of the *full* Lennard-Jones potential, $V_{\mathrm{LJ}}(r)$ that has a minimum value $V_{\mathrm{LJ}}(r_{\mathrm{min}}) = -\varepsilon$. The chain

connectivity was modeled by employing the finite extension nonlinear elastic (FENE) potential [16], using the same parameter values as in the simulation of normal star polymers [17,18]. The monomer mass m, the energy ε and the length σ_{LJ} are assigned the value unity, defining thereby the characteristic time $\tau = m\sigma_{\mathrm{LJ}}^2/\varepsilon$ and the dimensionless temperature $T^* = k_B T/\varepsilon$, where k_B is Boltzmann's constant. The equations of motion were integrated using the velocity form of Verlet's algorithm [19], whereas the temperature was fixed by applying a Langevin thermostat [20]. We measured the radius of gyration R_g of the molecules, the radial distribution function $g_t(r)$ between the terminal monomers, and the expectation value E_t of the interaction between the terminal groups, with $E_t = \langle \sum_{i=1}^{f} \sum_{j>i} V_{\mathrm{LJ}}(|\mathbf{t}_i - \mathbf{t}_j|)\rangle$, where $\langle \cdots \rangle$ denotes a statistical average and $\mathbf{t}_i$ stands for the position vector of the end monomer of the ith chain.

We considered temperatures between $T^* = 0.01$ and $T^* = 1.2$. For $T^* \gtrsim 0.2$, we found that the micelle configuration is similar to that of a star polymer without attractive ends, i.e., the *sb* configuration. A morphological transition of the micelles takes place upon lowering the temperature. In Fig. 1 we show the probability distribution function $P(E_t)$ for the end-monomer interaction energy E_t for the case $f = 3$, for different T^* and N values. Let us focus on $N = 10$. At $T^* = 1.0$, Fig. 1(a), $P(E_t)$ shows almost all the events around $E_t = 0$, meaning that in the vast majority of configurations the end-monomers are far apart, so that the attractions are vanishing. For $T^* = 0.2$, Fig. 1(b), $P(E_t)$ takes a bimodal form with two peaks, one at $E_t = 0$ and one at $E_t = -\varepsilon$. The latter corresponds to a conformation in which two chains are end attached, with their terminal monomers at a distance r_{min}, whereas the third chain is still free (intermediate configuration). Note that the molecule does fluctuate between the two conformations, as witnessed both by the bimodal character of the probability distribution and by the nonvanishing values of $P(E_t)$ for $-\varepsilon < E_t < 0$. Upon further lowering of the temperature at $T^* = 0.1$, Fig. 1(c), $P(E_t)$ develops a peak at $E_t = -3\varepsilon$: now *all three* terminal monomers are confined at a distance r_{min} from each other. This is the state in which the micelle has aggregation points at both ends WM conformation. The trend described above persists for $N = 50$. However, in each panel we can notice a higher probability to have association among chains by decreasing N. We further found a considerable sharpening of the peak at $E_t = -3\varepsilon$ for lowered temperatures, since fluctuations around the ground state are getting more suppressed.

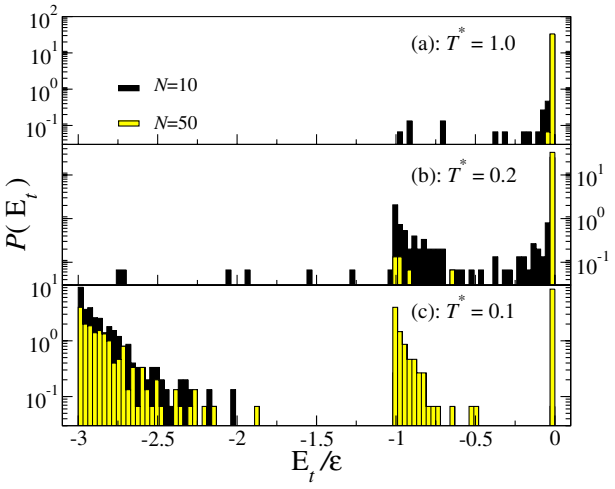

FIG. 1 (color online). The probability distribution function $P(E_t)$ obtained from simulations of $f = 3$ telechelic micelles carrying $N = 10, 50$ monomers per arm (logarithmic scale).

Similar results have been found for the cases $f = 2$, 4, and 5. At fixed N, the probability of chain association grows increasing f. The minimum value of E_t for $f = 2$ is $-\varepsilon$ and for $f = 4$ it is -6ε, corresponding to a WM configuration in which *every* end monomer is arranged at the vertices of a regular tetrahedron of edge length r_{min}. Because of geometrical constraints, for $f = 5$ it is not possible to have all five end monomers at contact with each other; the minimum value for E_t is -9ε in this case, corresponding to the arrangement of the terminal segments on the vertices of *two* regular tetrahedra of edge length r_{min}, which share a common face.

The temperature dependence of the gyration radius R_g for fixed $N = 10$ and different f values is shown in the main plot of Fig. 2. At high temperatures, R_g has a plateau that corresponds to the *sb* case and scales as $f^{1/5}N^{3/5}$ [21]. As T^* is lowered, we find a rapid decrease of R_g within a narrow temperature range and a saturation to a lower plateau value that corresponds to the size of the WM configuration. The attachment of the terminal monomers leads to a shrinking of the molecule, in agreement with the experimental findings of collapsed soft-sphere conformations [4]. The WM configuration persists to higher T^* values upon increasing the functionality f, a trend that can be attributed to the increasingly strong attractive-energy contributions to the WM free energy as f grows. In the inset of Fig. 2 we show the terminal-segment radial distribution function for the various f values at $T^* = 0.1$, where the WM conformation is stable and compare it with the one obtained for $f = 3$ at $T^* = 1.0$, where the micelles assume an *sb* conformation. The aggregation of the end monomers is clearly witnessed by the high peak at $r = r_{\mathrm{min}}$, which is present at $T^* = 0.1$, as opposed by the flat shape of $g_t(r)$ at $T^* = 1.0$. The double peak for the case $f = 5$ arises from the arrangement of the terminal monomers at the vertices of two tetrahedra. The most distant vertices of the two are separated by a distance $\sqrt{8/3}r_{\mathrm{min}}$, at which indeed the second peak in $g_t(r)$ shows up.

For the theoretical analysis, we consider the *sb* and WM configurations and put forward a scaling theory to determine the free energy F of each and find the stable one. The excluded-volume parameter v is set to unity ($v \cong \sigma_{\mathrm{LJ}}^3$). In the case of the *sb* configuration, the free energy is entirely entropic in nature and can be expressed as a sum of the

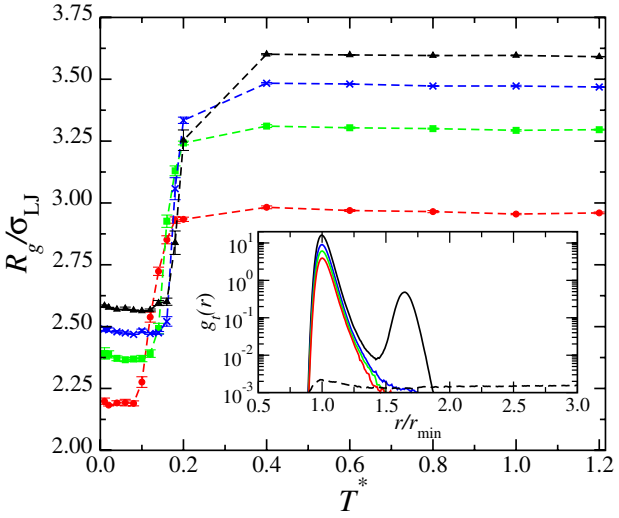

FIG. 2 (color online). Temperature dependence of R_g obtained by MD of telechelic micelles with $N = 10$. From top to bottom: $f = 5$ (black), $f = 4$ (blue), $f = 3$ (green), and $f = 2$ (red). Inset: the end monomer radial distribution function $g_t(r)$ obtained from MD at $T^* = 0.1$ (solid curves); the sequence from top to bottom is the same as those in the main plot. The dashed line is $g_t(r)$ for $f = 3$ and $T^* = 1.0$. For clarity, each curve has been multiplied by a different constant.

elastic and excluded-volume contributions. For a single chain, minimization of this sum with respect to the chain radius R_g leads to the scaling laws $R_g \sim N^{3/5}$ and $F \sim k_B T N^{1/5}$. For high-functionality star polymers, Flory theory can be improved in order to better take into account the interchain correlations by invoking the blob model of Daoud and Cotton [21,22]. For the small f values at hand, we envision instead each chain as a blob of radius $\sim R_g$ that occupies a solid angle $4\pi/f$. Accordingly, the total free energy of the *sb* configuration is approximated by $F_{sb} = k_B T f N^{1/5}$. The attractive contribution of the terminal monomers is very small, since the latter are far apart in the *sb* state, and it can thus be ignored.

In the WM configuration, there are two accumulation points: the first is the point in which the chains are chemically linked and the second is at the other end, at which the end monomers stick together. In order to properly take into account the monomer correlations within the macromolecule [23], we employ a blob model to estimate the excluded-volume contributions to the free energy F_{WM} [10,24]. A schematic representation of the watermelon and the associated blob model are shown in Fig. 3; the WM is thereby modeled as a double cone. With r_0 and l being the radius and height of the cone that contains n_b blobs of a single chain, we obtain

$$\frac{F_{WM}}{k_B T} = \frac{3}{2} f \frac{r_0^2 + l^2}{N} + 2 f n_b + E_{attr}. \qquad (1)$$

The first term at the right-hand side of Eq. (1) above is the stretching contribution of f chains, each having an extension $\sqrt{r_0^2 + l^2}$. The second is the excluded-volume cost and arises from the total number of $2fn_b$ blobs, each contributing an amount $k_B T$ [10,23,24]. Finally, the third term is the attractive-energy contribution arising from the total number of contacts between terminal monomers. Accordingly, $E_{attr} = -f(f-1)/(2T^*)$ for $f = 2$, 3, and 4, whereas $E_{attr} = -9/T^*$ for $f = 5$. The blobs are close packed within each cone, hence

$$\frac{l}{\cos(\alpha/2)} = D \sum_{n=0}^{n_b - 1} \left(\frac{1 + \sin(\alpha/2)}{1 - \sin(\alpha/2)} \right)^n, \qquad (2)$$

where $\alpha = \arctan(r_0/l)$ is the cone opening angle and D is the diameter of the first, smallest blob, taken equal to the monomer size. The polymerization N is obtained by summing over the monomers of all blobs of a chain, taking into account that a blob of size b contains $N_b \sim b^{5/3}$ monomers. This yields

$$N(r_0, l) = 2D^{5/3} \sum_{n=0}^{n_b - 1} \left(\frac{1 + \sin(\alpha/2)}{1 - \sin(\alpha/2)} \right)^{(5n/3)}. \qquad (3)$$

We solved Eqs. (2) and (3) numerically to express n_b and l in terms of r_0 and then we minimized numerically F_{WM} with respect to r_0 using Eq. (1). We found that the cone angle α between two arms increases rapidly with N for small N values: for $5 \lesssim N \lesssim 20$ it changes from 20° to 40°. This trend reflects the physical difficulty for the chains to form an aggregate for short chains, due to strong steric hindrance at the star center. Once the excluded-volume interactions are balanced, the angle increases slowly, by about 5° for $25 \lesssim N \lesssim 400$.

Comparing the minimized free energies F_{WM} with F_{sb}, we obtained the *transition* temperature between *sb* and WM as a function of N. In Fig. 4 we show the T vs N transition lines, separating the WM-state (below) from the *sb* one (above). The "critical number" N_c increases with decreasing T^* and the transition temperature increases with f as long as $f \leq 5$, so that the entropic penalty is not too high while the energetic gain from the multiple attraction grows. Stated otherwise, for fixed N the theoretical model gives evidence to a stronger stability of the WM configuration on increasing f and lowering the temperature. On the other hand, keeping f and T^* fixed, the *sb* configura-

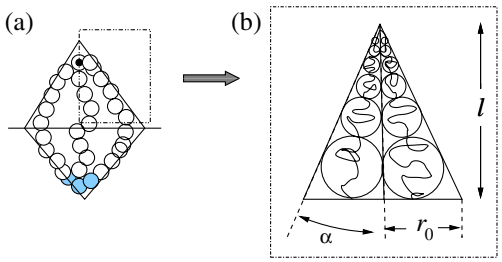

FIG. 3 (color online). (a) Schematic representation of a WM with $f = 3$, modeled as a double cone of half-chains; (b) the corresponding blob model of two arbitrary arms.

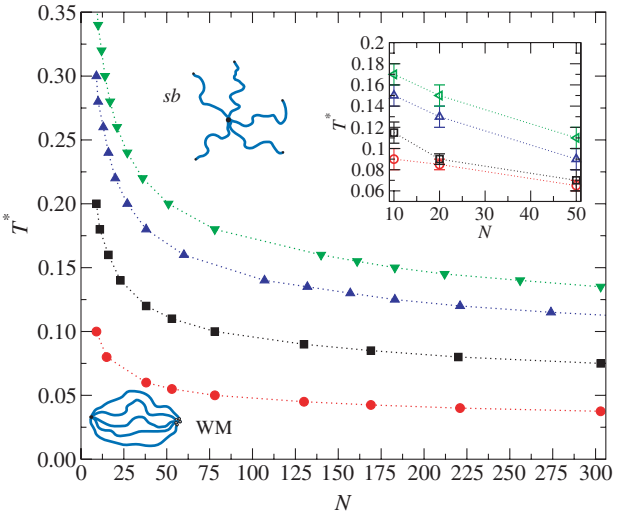

FIG. 4 (color online). Temperature versus N diagram corresponding to the *sb*- and WM-morphological transitions of telechelic micelles. Main figure: theoretical results. Inset: MD results. From bottom to top (full/empty symbols): $f = 2$ (circle), $f = 3$ (square), $f = 4$ (triangle up), $f = 5$ (triangle down).

tion is stable above a certain value of N_c. The dependence of the repulsive contribution in the free energy on the number of monomers is not trivial: increasing N, the number of blobs n_b increases and so does the contribution due to the excluded-volume interaction. The entropic contribution is proportional to r_0^2, which increases with N, and to $1/N$. The balance between all these terms in Eq. (1) determines the stable micelle conformation: it is physically more expensive for the molecule to assume a WM configuration the lower f and the higher N is. N_c decreases rapidly with T^* and the WM state becomes unstable at $T^* \gtrsim 0.3$ for all f values considered. In the inset of Fig. 4 we show the corresponding MD results for moderate N, in analogy of experimental systems [14]: notice the nice agreement with the theoretical prediction trends. The transition temperature is overestimated in theory, reflecting the mean-field nature of the latter. Along the lines put forward in this Letter we considered also intermediate configurations in which only a partial association of arms takes place (i.e., partial watermelons), akin to those seen for block-copolymer stars with $f = 12$ in the simulation study of Ref. [8]. Such configurations are unstable with respect to WM and *sb* ones, but they are expected to be dominant as f further increases, due to the very high entropic penalty inherent to a complete intramolecular association. Simulations for $f = 3$, $N = 100$, and $N = 200$ suggest that the transition temperature drops very rapidly with N, reaching thus values that are unphysically low for the relevant experimental systems [14].

We studied the dependence of the equilibrium conformations of telechelic stars on the temperature, arm number, and number of monomers. The system presents a stable, watermelon configuration for low temperatures that opens up as T grows. The possibility to form an empty-collapsed structure opens the way to biomedical applications such as WM vehicles able to encapsulate drugs and/or to inhibit the adsorption of substance on the body (e.g., lipids). The dynamical properties of such aggregates in solution will have unusual characteristics: at low temperatures and near the overlap concentration, various types of gels can appear, owing their viscosity either to transient network formation or to the existence of entangled loops. An understanding of the changes in the micelle conformations is a relevant starting point, aiming at gaining control over the supramolecular structural and dynamical properties of the system [25], and targeting specific applications.

We thank W. Russel and D. Vlassopoulos. C. M. thanks the Düsseldorf EF for financial support. This work was supported by the DFG within the SFB-TR6 and by the Marie Curie European Network MRTN-CT-2003-504712.

[1] M. Muthukumar *et al.*, Science **277**, 1225 (1997).
[2] *Theoretical Challenges in the Dynamics of Complex Fluids*, NATO ASI Vol. 339 (Kluwer, London, 1997).
[3] M. Pitsikalis *et al.*, Macromolecules **29**, 179 (1996).
[4] D. Vlassopoulos *et al.*, J. Chem. Phys. **111**, 1760 (1999).
[5] F. Clément *et al.*, Macromolecules **33**, 6148 (2000).
[6] Yu. D. Zaroslov *et al.*, Macromol. Chem. Phys. **206**, 173 (2005).
[7] F. Ganazzoli *et al.*, Macromol. Theory Simul. **10**, 325 (2001).
[8] R. Connolly *et al.*, J. Chem. Phys. **119**, 8736 (2003).
[9] A. N. Semenov *et al.*, Macromolecules **28**, 1066 (1995).
[10] A. G. Zilman and S. A. Safran, Eur. Phys. J. E **4**, 467 (2001).
[11] X.-X. Meng and W. B. Russel, Macromolecules **36**, 10 112 (2003).
[12] S. R. Bhatia and W. B. Russel Macromolecules **33**, 5713 (2000).
[13] U. Batra *et al.*, Macromolecules **30**, 6120 (1997).
[14] D. Vlassopoulos *et al.*, Macromolecules **33**, 9740 (2000).
[15] M. Pitsikalis and N. Hadjichristidis, Macromolecules **28**, 3904 (1995).
[16] M. J. Stevens and K. Kremer, Phys. Rev. Lett. **71**, 2228 (1993).
[17] G. S. Grest *et al.*, Macromolecules **20**, 1376 (1987).
[18] G. S. Grest *et al.*, Adv. Chem. Phys. **XCIV**, 67 (1996).
[19] M. P. Allen and D. J. Tildesley, *Computer Simulation of Liquids* (Oxford University, Oxford, 1987).
[20] K. Kremer and G. S. Grest, J. Chem. Phys. **92**, 5057 (1990).
[21] M. Daoud and J. P. Cotton, J. Physique **43**, 531 (1982).
[22] T. A. Witten and P. A. Pincus, Macromolecules **19**, 2509 (1986).
[23] A. Yu. Grosberg and A. R. Khokhlov, *Statistical Physics of Macromolecules* (AIP, New York, 1994).
[24] P. G. de Gennes, *Solid State Physics, Supplement 14: Liquid Crystals* (Academic, New York, 1978).
[25] G. Arya and A. Z. Panagiotopoulos, Phys. Rev. Lett. **95**, 188301 (2005).